Crossed-beam reaction of carbon atoms with hydrocarbon molecules. III: Chemical dynamics of propynylidyne (l-C_3H; $X\ ^2\Pi_j$) and cyclopropynylidyne (c-C_3H; $X\ ^2B_2$) formation from reaction of $C(^3P_j)$ with acetylene, $C_2H_2(X\ ^1\Sigma_g^+)$

R. I. Kaiser, C. Ochsenfeld, M. Head-Gordon, Y. T. Lee,[a] and A. G. Suits
Department of Chemistry, University of California, Berkeley, California 94720, and Chemical Sciences Division, Berkeley National Laboratory, Berkeley, California 94720

(Received 3 October 1996; accepted 24 October 1996)

The reaction between ground state carbon atoms, $C(^3P_j)$, and acetylene, $C_2H_2(X\ ^1\Sigma_g^+)$, is studied at three collision energies between 8.8 and 45.0 kJ mol^{-1} using the crossed molecular beams technique. Product angular distributions and time-of-flight spectra of C_3H at $m/e=37$ are recorded. Forward-convolution fitting of the data yields weakly polarized center-of-mass angular flux distributions decreasingly forward scattered with respect to the carbon beam as the collision energy rises from 8.8 to 28.0 kJ mol^{-1}, and isotropic at 45.0 kJ mol^{-1}. Reaction dynamics inferred from the experimental data and *ab initio* calculations on the triplet C_3H_2 and doublet C_3H potential energy surface suggest two microchannels initiated by addition of $C(^3P_j)$ either to one acetylenic carbon to form *s-trans* propenediylidene or to two carbon atoms to yield triplet cyclopropenylidene via loose transition states located at their centrifugal barriers. Propenediylidene rotates around its B/C axis and undergoes [2,3]-H-migration to propargylene, followed by C–H bond cleavage via a symmetric exit transition state to l-$C_3H(X\ ^2\Pi_j)$ and H. Direct stripping dynamics contribute to the forward-scattered second microchannel to form c-$C_3H(X\ ^2B_2)$ and H. This contribution is quenched with rising collision energy. The explicit identification of l-$C_3H(X\ ^2\Pi_j)$ and c-$C_3H(X\ ^2B_2)$ under single collision conditions represents a one-encounter mechanism to build up hydrocarbon radicals in the interstellar medium and resembles a more realistic synthetic route to interstellar C_3H isomers than hitherto postulated ion–molecule reactions. Relative reaction cross sections to the linear versus cyclic isomer correlate with actual astronomical observations and explain a higher [c-C_3H]/[l-C_3H] ratio in the molecular cloud TMC-1 ($\approx$1) as compared to the circumstellar envelope surrounding the carbon star IRC+10216 ($\approx$0.2) via the atom-neutral reaction $C(^3P_j)+C_2H_2(X\ ^1\Sigma_g^+)$. © *1997 American Institute of Physics.* [S0021-9606(97)01305-6]

I. INTRODUCTION

Linear and cyclic C_3H, i.e., propynylidyne (l-C_3H) and cyclopropynylidyne (c-C_3H), Fig. 1, are ubiquitous in the interstellar medium (ISM) and hold high fractional abundances up to 10^{-9} relative to atomic hydrogen. l-C_3H was detected in 1985 by Thaddeus *et al.* via microwave spectroscopy toward the dark Taurus molecular cloud 1 (TMC-1) and the carbon star IRC+10216.[1,2] Two years later, Yamamoto *et al.*[3] identified rotational transitions of the cyclic isomer in TMC-1 prior to laboratory synthesis via radio frequency discharge of He/CO/C_2H_2 mixtures. Interstellar reaction networks postulate their formation via successive ion–molecule reactions, radiative associations, and dissociative recombinations (reactions 1–4[4–6] or reactions 5–7[7]):

$$C_2H_2+C^+\rightarrow l/c\text{-}C_3H^++H, \tag{1}$$

$$l/c-C_3H^++H_2\rightarrow c\text{-}C_3H_3^++h\nu, \tag{2}$$

$$l/c-C_3H_3^++e^-\rightarrow l/c\text{-}C_3H+2H, \tag{3}$$

$$\rightarrow l/c\text{-}C_3H+H_2, \tag{4}$$

$$C_2H_4+C^+\rightarrow c-C_3H_3^++H \tag{5}$$

$$\rightarrow l/c\text{-}C_3H_2^++H_2 \tag{6}$$

$$l/c-C_3H_2^++e\rightarrow l/c\text{-}C_3H+H. \tag{7}$$

Very recently, however, crossed molecular beam reactions of atomic carbon in its ^3P_j electronic ground state with acetylene (reaction 8[8]), ethylene (reaction 9[9]), and methylacetylene (reaction 10[10]) established the carbon–hydrogen exchange channel to tricarbon hydride, the propargyl radical, and butatrienyl/α-ethinylvinylidene as an alternative pathway to synthesize neutral species:

$$C(^3P_j)+C_2H_2\rightarrow C_3H+H, \tag{8}$$

$$C(^3P_j)+C_2H_4\rightarrow l\text{-}C_3H_3+H, \tag{9}$$

$$C(^3P_j)+CH_3CCH\rightarrow n\text{-}C_4H_3+H. \tag{10}$$

Although our preliminary studies on the $C(^3P_j)/C_2H_2$ system could not identify the C_3H isomer,[8] this mechanism opens a versatile route to form extremely reactive hydrocarbon radicals via atom-neutral reactions under single collision conditions in the ISM and does not require reaction chains of successive binary encounters under interstellar conditions with reactant number densities as low as 10^{-4} cm^{-3}.

Despite the key role of the C_3H system in understanding the competition between ion–molecule reactions and atom-

[a]Present address: Academia Sinica, Nankang, Taipei, 11529, Taiwan.

Downloaded¬12¬May¬2006¬to¬128.171.55.146.¬Redistribution¬subject¬to¬AIP¬license¬or¬copyright,¬see¬http://jcp.aip.org/jcp/copyright.jsp

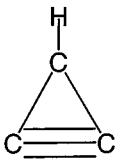

(1)

(2)

FIG. 1. Schematic C_{2v} and $C_{\infty v}$ structures of the *c*- and *l*-C_3H isomer (1) and (2) as derived from microwave spectra.

neutral chemistry in the ISM, the C_3H potential energy surface (PES) is poorly characterized. *c*-C_3H in its $^2B_2$ electronic ground state holds the global minimum and resembles a prolate asymmetric top of C_{2v} symmetry with rotational constants $A=1.48$ cm^{-1}, $B=1.1$ cm^{-1}, and $C=0.64$ cm^{-1}.[11–18] The unpaired electron is delocalized over the carbon skeleton as reflected in almost identical carbon–carbon bond lengths of r(C–CH)=1.3739 Å, and r(C–C)=1.3771 Å determined via microwave spectra, as well as the nearly uniform *p*-character of the *A*-axis based carbon atom of 31.8% versus a 20.4% contribution from the two symmetric C atoms.[19] This electron delocalization gives rise to a spin-orbit splitting of 0.32 kJ mol^{-1}.[19] The presence of a low-lying excited A^2A_1 electronic state about 120 kJ mol^{-1} above the ground state induces a pseudo Jahn–Teller effect, but its magnitude is not strong enough to distort the carbon skeleton to a reduced C_s symmetry.[20]

The linear isomer in its doubly degenerate $^2\Pi_{1/2}$ electronic ground state was thought to be 1.3–28.2 kJ mol^{-1} less stable than *c*-C_3H.[21–24] Laboratory as well as interstellar microwave spectra indicate that *l*-C_3H belongs to the $C_{\infty v}$ point group and has a rotational constant $B=0.37$ cm^{-1}.[21–24] Spin-orbit coupling is less efficient in this system as compared to the cyclic one, and the $^2\Pi_{3/2}$ state is separated by only 0.18 kJ mol^{-1} from the true electronic ground state.[21–24] In strong contrast to *c*-C_3H, the unpaired electron is predominantly confined to 90% to the *p* atom orbital of the terminal carbon atom, and delocalized to only 10% over a π molecular orbital (MO).[21–24] Distinct carbon–carbon lengths of r(HC–C) =1.2539 Å and r(HCC–C)=1.3263 Å support this finding. Further, the C–H distance of 1.0171 Å is shorter than a typical acetylenic carbon–hydrogen bond with 1.0605 Å and is interpreted in terms of a large amplitude motion of the doubly degenerate ν_4-CCH bending mode. Due to the ν_4 interaction with the $X\ ^2\Pi_{1/2}$ state (Renner–Teller effect), its vibration energy ranges only 0.3 kJ mol^{-1} above the $X\ ^2\Pi_{1/2}$ state.[23,24]

Previous mechanistic information on the C(^3P_j)/C_2H_2 system were derived from bulk experiments at 293 K[25] and indicate the reaction proceeds within orbiting limit, i.e., a dominating C_6 dispersions interaction term and chemical dynamics invariant with respect to the C_2H_2 geometry.[26] Herbst *et al.*[27] reproduced Husain *et al.*'s[25] rate constant with the orbiting framework assuming only one third of the trajectories lead to products. This conclusion correlates with Takahashi and Yamashita's *ab initio* calculations and suggests that the initially triply degenerate surface splits into one attractive and two repulsive ones as the reactants approach.[28] Reaction products were first identified via a crossed beam study of (8) under single collision conditions as tricarbon hydride, C_3H, and atomic hydrogen.[8]

In this paper, we extend our preliminary investigations on the C(^3P_j)/C_2H_2 system and elucidate the energy dependent chemical dynamics of the atom-neutral reaction C(^3P_j)/C_2H_2($X\ ^1\Sigma_g^+$) under single collision conditions at collision energies between 8.8 and 45.0 kJ mol^{-1}. The direct measurement of product velocity and angular distributions identify the primary reaction channel(s) and acquire dynamical information on elementary steps of the reaction. State-of-the-art *ab initio* calculations on the doublet C_3H and triplet C_3H_2 surfaces supplement our experimental data (compare Refs. 29–30). Together they reveal possible reaction pathways to interstellar C_3H isomers, C_3H radicals postulated in chemical vapor deposition (CVD) processes to synthetic diamonds,[31,32] as well as trapped C_3H_2 intermediates in C_2H_2/O_2 flames.[33]

II. EXPERIMENTAL SETUP AND DATA ANALYSIS

Since atomic carbon is tetravalent in closed shell molecules, formation of chemically stable species in the very first encounter is highly unlikely, and experiments must be performed under single collision conditions to identify the primary reaction products. These requirements are achieved here using a universal crossed molecular beam apparatus described in Ref. 34 in detail. A pulsed supersonic carbon beam was generated via laser ablation of graphite at 266 nm.[35] The 30 Hz, 35–40 mJ output of a Spectra Physics GCR-270-30 Nd:YAG laser is focused onto a rotating carbon rod. Ablated carbon atoms are seeded into neon or helium carrier gas released by a Proch–Trickl pulsed valve operating at 60 Hz and 80 μs pulses with 4 atm backing pressure. This setup generates C(^3P_j) within the velocity regime 800–3000 ms^{-1},[35] C(^3P_j/$^1D_2$) between 3000 and 3300 ms^{-1},[36] and solely C($^1D_2$) in the free ablation mode yielding velocities between 3300 and 5500 ms^{-1}.[36] A four slot chopper wheel selects a 7.0 μs segment of the seeded carbon beam. Table I compiles the experimental beam conditions. The carbon beam at 45.0 kJ mol^{-1} contains contributions of C($^1D_2$) atoms, whose reaction dynamics are the subject of a forthcoming article. Since excited electronic state of C_2 and C_3 are expected as well, but no fragmentation patterns are available, the composition of the carbon beam as well as the flux factor are extremely speculative at this collision energy and are therefore excluded from Table I.

The pulsed carbon and a continuous acetylene beam at 550±12 Torr backing pressure pass through skimmers and cross at 90° in the interaction region of the scattering chamber. Products were detected in the plane of the beams using a rotable quadrupole mass spectrometer with electron-impact ionizer at different laboratory angles steps between 5.0° and 60.0° with respect to the carbon beam. Time-of-flight spectra (TOF) were recorded choosing a channel width of 7.5 μs. The velocity of the supersonic carbon beam was monitored

Downloaded¬12¬May¬2006¬to¬128.171.55.146.¬Redistribution¬subject¬to¬AIP¬license¬or¬copyright,¬see¬http://jcp.aip.org/jcp/copyright.jsp

TABLE I. Experimental beam conditions and 1σ errors averaged over the experimental time: most probable velocity v_0, speed ratio S, most probable relative collision energy, E_{coll}, center-of-mass angle, θ_{CM}, composition of the carbon beam, and flux factor $f_v = n(\text{C}) * n(\text{C}_2\text{H}_2) * v_r$ in relative units, with the number density of the ith reactant n_i and the relative velocity v_r ?: no information available; see text for explanation.

Beam	v_0, ms^{-1}	S	E_{coll} (kJ mol^{-1})	θ_{CM}	C_1:C_2:C_3	f_v
$C(^3P_j)$/Ne	1180±54	6.0±0.5	8.8±0.4	57.8±1.2	1:0.7:2.5	1.0
$C(^3P_j)$/He	2463±88	4.6±0.5	28.0±2.0	37.3±0.9	1:0.14:0.25	6.2±2.4
$C(^3P_j)$/He	3196±106	2.6±0.5	45.0±3.0	30.4±0.8	?	?
C_2H_2	866±5	9.3±0.6	…	…	…	…

frequently and minor velocity drifts corrected by adjusting the laser pulse delay within ±1.0 μs. To calibrate fluctuating carbon beam intensities and mass dial settings at the quadrupole controller, reference angles were chosen at 60.0° (8.8 kJ mol^{-1}), 37.5° (28.0 kJ mol^{-1}), and 30.0° (45.0 kJ mol^{-1}).

Kinematic information are extracted by fitting the TOF spectra and the product angular distribution in the laboratory frame using a forward-convolution routine.[37] This iterative approach initially guesses the angular flux distribution $T(\theta)$ and the translational energy flux distribution $P(E_T)$ in the center-of-mass system (CM) assuming mutual independence. Laboratory TOF spectra and the laboratory angular distributions (LAB) are then calculated from these $T(\theta)$'s and $P(E_T)$'s convoluted over the apparatus functions to obtain simulations of the experimental data.

III. *AB-INITIO* CALCULATIONS

All *ab initio* results presented in this paper have been computed at the CCSD(T) level (single- and double-excitation coupled cluster with a perturbational estimate of triple excitations),[38–41] based on unrestricted Hartree–Fock (UHF) wave functions. The ACES II program package was

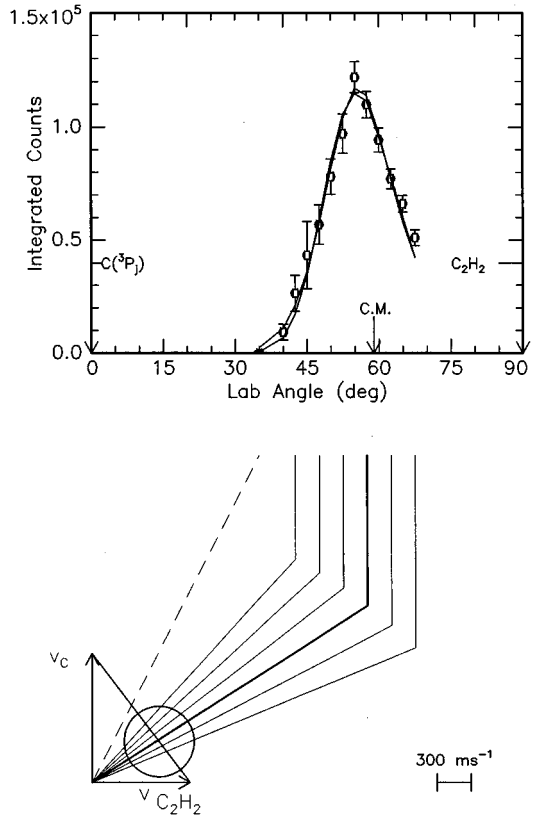

FIG. 2. Lower: Newton diagram for the reaction $C(^3P_j)+C_2H_2(X\ ^1\Sigma_g^+)$ at a collision energy of 8.8 kJ mol^{-1}. The circle stands for the maximum center-of-mass recoil velocity of the C_3H product in the CM reference frame. Upper: Laboratory angular distribution of C_3H at $m/e=37$. Circles and 1σ error bars indicate experimental data, the solid lines the calculated distribution of the upper and lower carbon beam velocity (Table I). C.M. designates the center-of-mass angle. The solid lines originating in the Newton diagram point to distinct laboratory angles whose TOFs are shown in Fig. 5. The dashed line denotes the experimentally determined signal cutoff at 35°.

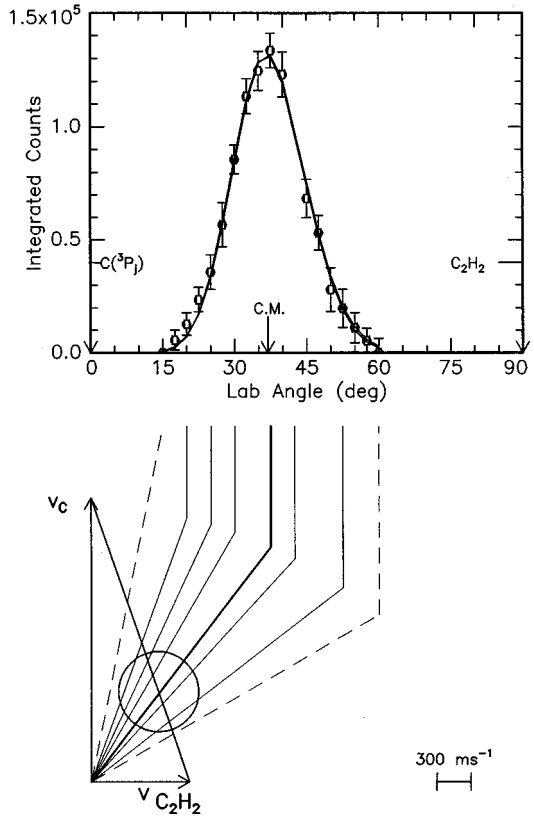

FIG. 3. Lower: Newton diagram of the reaction $C(^3P_j)+C_2H_2(X\ ^1\Sigma_g^+)$ at a collision energy of 28.0 kJ mol^{-1}. The circle stands of the maximum center-of-mass recoil velocity of the C_3H product in the CM reference frame. Upper: Laboratory angular distribution of C_3H at $m/e=37$. Circles and 1σ error bars indicate experimental data, the solid lines the calculated distribution for the upper and lower carbon beam velocity (Table I). C.M. designates the center-of-mass angle. The solid lines originating in the Newton diagram point to distinct laboratory angles whose TOFs are shown in Fig. 6. Dashed lines denote the experimentally determined signal cut-offs at 15 and 60°.

Downloaded¬12¬May¬2006¬to¬128.171.55.146.¬Redistribution¬subject¬to¬AIP¬license¬or¬copyright,¬see¬http://jcp.aip.org/jcp/copyright.jsp

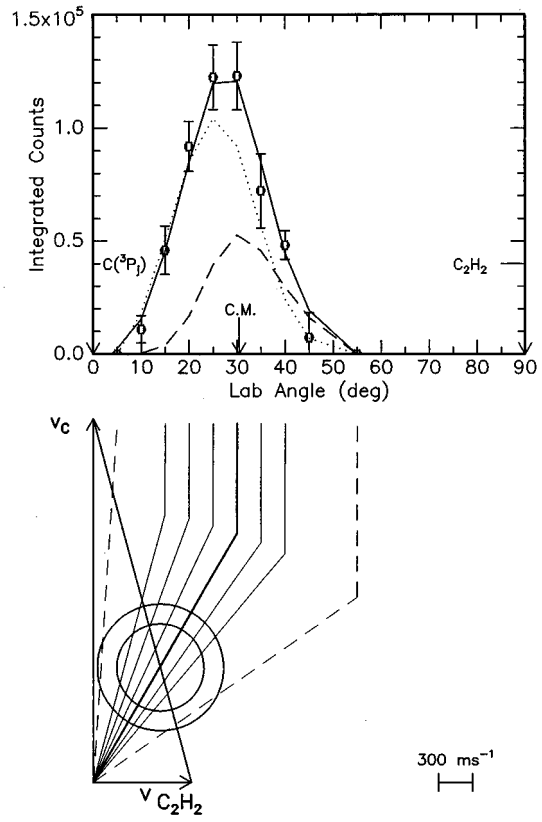

FIG. 4. Lower: Newton diagram for the reaction $C(^3P_j)+C_2H_2(X\ ^1\Sigma_g^+)$ at a collision energy of 45.0 kJ mol^{-1}. The circles stand for the maximum center-of-mass recoil velocity of the C_3H product in the CM reference frame from reaction of acetylene with $C(^1D_2)$ (outer circle) and $C(^3P_j)$ (inner circle). Upper: Laboratory angular distribution of C_3H at $m/e=37$. Circles and 1σ error bars indicate experimental data, the solid lines the sum of calculated distribution for the upper and lower carbon beam velocity from reaction of $C(^1D_2)$ (dotted line) and $C(^3P_j)$ (dashed line). C.M. designates the center-of-mass angle. The solid lines originating in the Newton diagram point to distinct laboratory angles whose TOFs are shown in Fig. 7. Dashed lines denote the experimentally determined signal cutoffs at 5° and 55°.

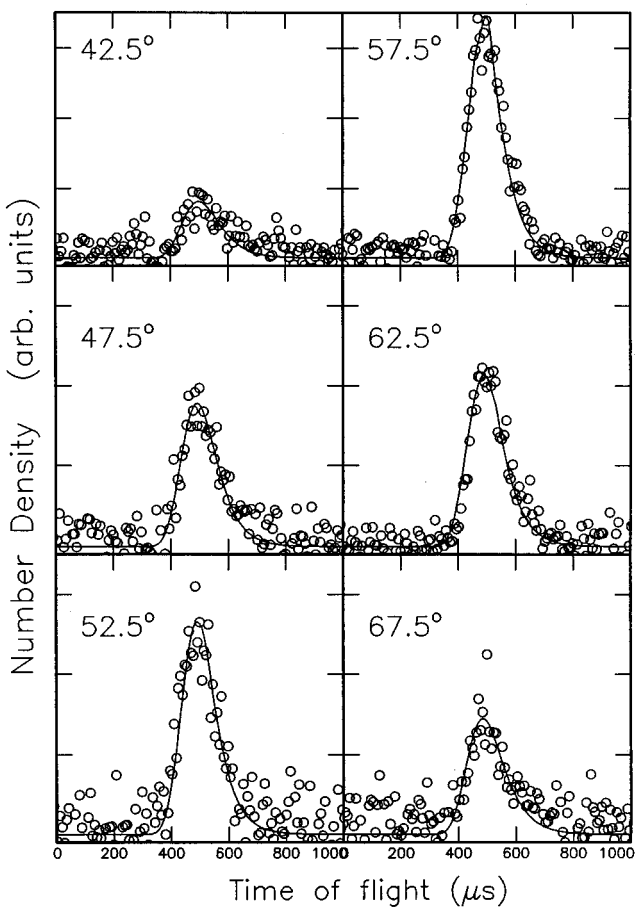

FIG. 5. Time-of-flight data at $m/e=37$ for indicated laboratory angles at a collision energy of 8.8 kJ mol^{-}. Open circles represent experimental data, the solid line the fit. TOF spectra have been normalized to the relative intensity at each angle.

used.[42–44] Stability of the zeroth-order self-consistent field (SCF) wave functions[44] has been checked, and spin contamination occurring in the SCF wave function (typically 2.40 for $\langle S^2\rangle$ in triplet states of C_3H_2) is mostly eliminated within the coupled cluster scheme. All structures were fully optimized at the CCSD(T) level. To characterize stationary points (local minima or saddle points), vibrational frequencies have been calculated numerically within the harmonic approximation using analytic CCSD(T) gradients. Geometries, vibrational frequencies, as well as zero-point energies have been computed for all isomers using a triple-zeta plus polarization basis set (TZP)[45] (H: $(5s1p)/[3s1p]$; C: $(10s6p1d)/[6s3p1d]$). Energy differences were obtained by single-point calculations with a quadruple-zeta double polarization (QZ2P)[45] basis (H: $(7s2p1d)/[4s2p1d]$; C: $(11s7p2d1f)/[6s4p2d1f]$) at the UCCSD(T)/TZP geometries. For some of the reaction energies a cc-pVQZ basis was used (H: $(6s3p2d1f)/[4s3p2d1f]$; C: $(12s6p3d2f1g)/[5s4p3d2f1g]$).[46] This approach is expected to yield standard reaction enthalpies with an accuracy of about 1–3 kJ mol^{-1}. The systematic *ab initio* investigations of the triplet C_3H_2 and doublet C_3H systems are described elsewhere in detail,[30] where methodical aspects, energies, energy differences, geometries, and vibrational frequencies are discussed extensively. Here, we focus on results necessary to supplement our experimental data.

IV. RESULTS

A. Reactive scattering signal

Reactive scattering signal was only observed at $m/e=37$, i.e., C_3H, cf. Figs. 2–7 and Table II. TOF spectra recorded at $m/e=36$ show identical patterns indicating that the energetically accessible, but spin forbidden channel 3 is closed. Endothermic exit channels 4–6 could not be opened at relative collision energies applied here. Additionally, no radiative association to C_3H_2 at $m/e=50$ or higher masses were observed.

B. Laboratory angular distributions (LAB) and TOF spectra

Figures 2–4 display the most probable Newton diagrams of the title reaction as well as the laboratory angular (LAB)

Downloaded¬12¬May¬2006¬to¬128.171.55.146.¬Redistribution¬subject¬to¬AIP¬license¬or¬copyright,¬see¬http://jcp.aip.org/jcp/copyright.jsp

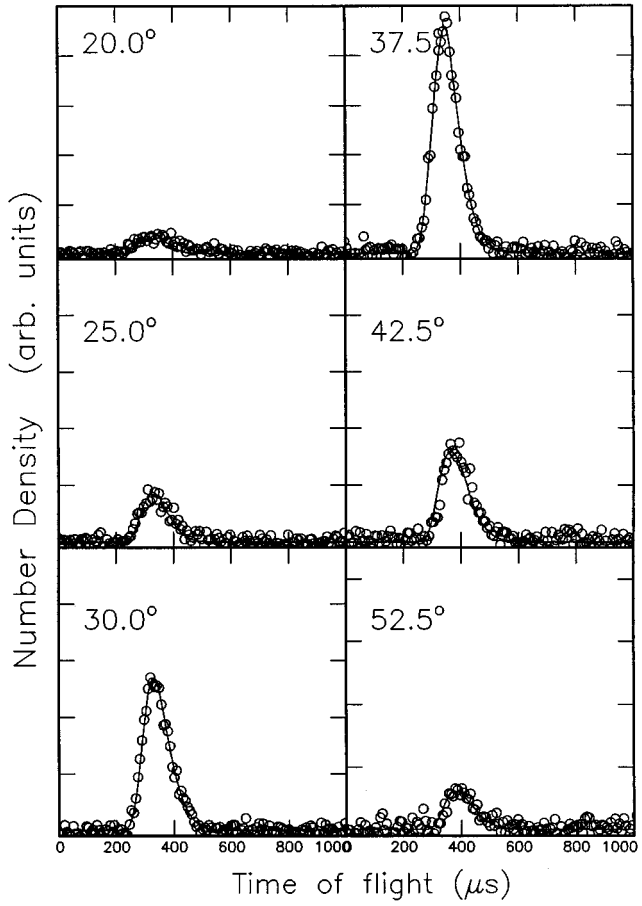

FIG. 6. Time-of-flight data at $m/e=37$ for indicated laboratory angles at a collision energy of 28.0 kJ mol^{-1}. Open circles represent experimental data, the solid line the fit. TOF spectra have been normalized to the relative intensity at each angle.

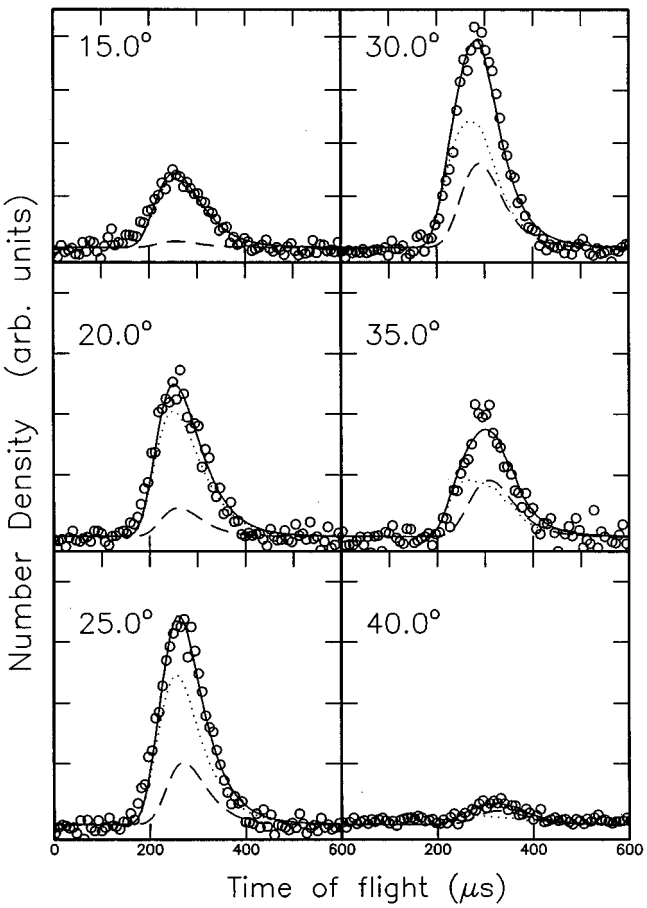

FIG. 7. Time-of-flight data $m/e=37$ for indicated laboratory angles at a collision energy of 45.0 kJ mol^{-1}. Open circles represent experimental data, the solid line the fit. Dotted lines show the contribution of C($^1D_2$) and dashed lines of C(^3P_j). TOF spectra have been normalized to the relative intensity at each angle.

distributions of the C_3H product at collision energies of 8.8, 28.0, and 45.0 kJ mol^{-1}. At the lowest applied collision energy, the LAB distribution peaks at 50.0°, slightly forward scattered with respect to the center of mass (CM) angle at 57.9°. As increased to 28.0 and 45.0 kJ mol^{-1}, the fits of both LAB distributions originating from the C(^3P_j) component reveal maxima at the CM angles of 37.3° and 30.4°, respectively. Since the enthalpies of formation of both C_3H isomers differ by about 7.5 kJ mol^{-1}, c.f. Sec. V A, the differentiation of c-C_3H versus l-C_3H based solely on limiting circles is not possible. However, the dashed lines originating in the Newton diagrams support the correct order-of-magnitude of the calculated reaction enthalpy even within the velocity spreads, since no reactive scattering signal was detected outside the thermodynamical limit. Further, the narrow range of the laboratory angular distribution of only 45.0° and the mass ratio of both departing C_3H and H fragments (37:1) suggest that the averaged translational energy release $\langle E_T \rangle$ is small as confirmed in our *ab initio* calculations of the reaction exothermicities, Table II. In addition, all center-of-mass translational energy distributions $P(E_T)$s are expected to peak near zero indicating a loose exit transition state from the decomposing C_3H_2 complex(es) to the products.

C. Center-of-mass translational energy distributions, $P(E_T)$

Figure 8 presents the translational energy distributions $P(E_T)$ and angular distributions $T(\theta)$ in the center-of-mass frame of the reaction C(^3P_j)+C_2H_2($X\ ^1\Sigma_g^+$)→C_3H+H. Best fits of TOF and LAB distributions were gained with $P(E_T)$s extending to a maximum translational energy release E_{max} of 20 kJ mol^{-1} (E_{coll}=8.8 kJ mol^{-1}), 43 kJ mol^{-1} (E_{coll}=28.0 kJ mol^{-1}), and 57 kJ mol^{-1} (E_{coll}=45.0 kJ mol^{-1}). Further, the most probable translational energy yields the order-of-magnitude of the barrier height in the exit channel. As expected from the LAB distributions, all $P(E_T)$s peak near zero, here between 5 and 16 kJ mol^{-1}. These findings suggest a nearly simple bond-rupture process via a loose exit transition state and a minor electron density reorganization from the decomposing C_3H_2 complex to the products. Finally, the average translational energy release obtained was 8.0±3.0 kJ mol^{-1} at E_{coll}=8.8 kJ mol^{-1}, 17.0±2.0 kJ mol^{-1} at E_{coll}=28.0 kJ mol^{-1}, and 23.0±4.0 kJ mol^{-1} at E_{coll}=45.0 kJ mol^{-1}.

Downloaded¬12¬May¬2006¬to¬128.171.55.146.¬Redistribution¬subject¬to¬AIP¬license¬or¬copyright,¬see¬http://jcp.aip.org/jcp/copyright.jsp

TABLE II. Thermochemistry of the reaction $C(^3P_j)+C_2H_2(X\ ^1\Sigma_g^+)$. Enthalpies of formations were taken from Ref. 36 (reactions 3–6) and present *ab initio* calculations (reactions 1–2).

No.	Exit channel	Free reaction enthalpy at 0 K, $\Delta_R G$ (0 K), kJ mol^{-1}
1	c-C_3H $(X\ ^2B_2)+H(^2S_{1/2})$	−8.6
2	l-$C_3H(X\ ^2\Pi_{1/2})+H\ (^2S_{1/2})$	−1.5
3	$C_3\ (X\ ^1\Sigma_g^+)+H_2(X\ ^1\Sigma_g^+)$	−127.0±5.0
4	$C_3\ (a\ ^3\Pi_u)+H_2(X\ ^1\Sigma_g^+)$	+73.5±5.0
5	$C_2H\ (X\ ^2\Sigma^+)+CH(X\ ^2\Pi_{1/2})$	+118.5±15.0
6	$CH_2\ (X\ ^3B_1)+C_2(X\ ^1\Sigma_g^+)$	+267.0±14.0

D. Center-of-mass angular distributions, $T(\theta)$

As the collision energy increases, the $T(\theta)$s show a decreasing total fraction of forward scattering from 27.0±3.0% (8.8 kJ mol^{-1}) via 7.0±3.0% (28.0 kJ mol^{-1}) to an isotropic distribution at 45.0 kJ mol^{-1} (Fig. 8). In strong coincidence, the intensity ratio of $T(\theta)$ at $\theta=0°$ to 180° drops from 2.6 ±0.3 via 1.2±0.2 to 1.0 with rising collision energy. These data eliminate an osculating complex as discussed in Refs. 9 and 10, but rather indicate two distinct microchannels. The first one is strongly forward scattered with respect to the carbon beam and shows a significant correlation of the initial and final orbital angular momentum **L** and **L**′ perpendicular to the initial and final relative velocity vectors **v** and **v**′. As the collision energy rises, this contribution is quenched. The collision energy invariant forward–backward symmetric $T(\theta)$ shape of the weakly polarized and isotropic microchannel 2 is either induced by a long-lived complex behavior of the decomposing C_3H_2 intermediate holding a lifetime longer than its rotational period[47,48] or alternatively via a symmetric C_3H_2 intermediate giving rise to a symmetric exit transition state.[9,10] Its weak polarization results from total angular momentum conservation and angular momentum disposal as discussed previously.[9,10] Since C_2H_2 is prepared in a supersonic expansion and the rotational state distribution peaks at only $2\hbar$ at a typical rotational temperature of 20–30 K, a classical treatment defines the total angular momentum **J** to

$$\mathbf{J}=\mathbf{L}'+\mathbf{j}'\approx\mathbf{L} \tag{11}$$

with the rotational angular momentum of the C_3H product **j**′. The maximum initial orbital angular momentum $L_{\max}$ can be approximated referring to bulk experiments which indicate the title reaction proceeds within orbiting limits.[25] Therefore, we calculate the maximum impact parameter $b_{\max}$ leading to reaction to $b_{\max}$(8.8 kJ mol^{-1})=3.6 Å, $b_{\max}$(28.0 kJ mol^{-1})=2.7 Å, and $b_{\max}$(45.0 kJ mol^{-1})=2.5 Å, and the maximum orbital angular momentum $L_{\max}$ to $L_{\max}$(8.8 kJ mol^{-1})=65±3$\hbar$, $L_{\max}$(28.0 kJ mol^{-1})=95±4$\hbar$, and $L_{\max}$(45.0 kJ mol^{-1})=111±5$\hbar$. Further, an upper limit of L' is estimated by choosing exit impact parameters to typical dimensions in feasible decomposing C_3H_2 complexes between 1.0 and 1.5 Å, cf. Sec. V A. This procedure yields L'(8.8 kJ mol^{-1})<10$\hbar$, L'(28.0 kJ mol^{-1})<15$\hbar$, and L'(45.0 kJ mol^{-1})<22$\hbar$. Since $L'<0.18\ L$, **L** and **L**′ are poorly coupled, and most of the total angular momentum channels into rotational excitation of the C_3H product on average to result in weakly polarized $T(\theta)$s.

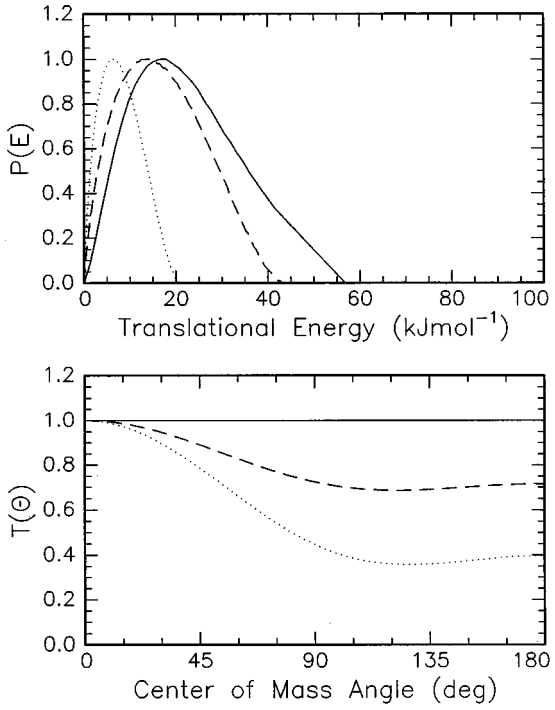

FIG. 8. Lower: Center-of-mass angular flux distributions for the reaction $C(^3P_j)+C_2H_2(X\ \Sigma_g^+)$ at collision energies of 8.8 (dotted line), 28.0 (dashed line), and 45.0 kJ mol^{-1} (solid line). Upper: Center-of-mass translational energy flux distributions for the reaction $C(^3P_j)+C_2H_2(X\ ^1\Sigma_g^+)$ at collision energies of 8.8 (dotted line), 28.0 (dashed line), and 45.0 kJ mol^{-1} (solid line).

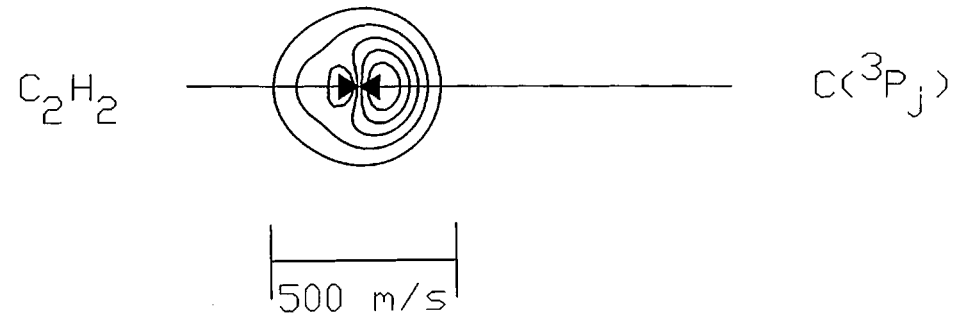

FIG. 9. Contour flux map distribution for the reaction $C(^3P_j)+C_2H_2(X\ ^1\Sigma_g^+)$ at a collision energy of 8.8 kJ mol^{-1}.

Downloaded¬12¬May¬2006¬to¬128.171.55.146.¬Redistribution¬subject¬to¬AIP¬license¬or¬copyright,¬see¬http://jcp.aip.org/jcp/copyright.jsp

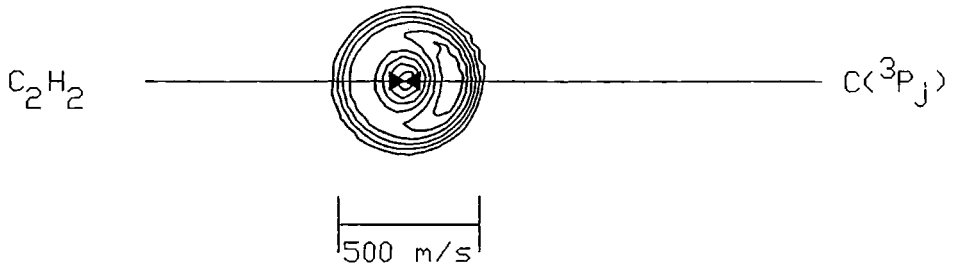

FIG. 10. Contour flux map distribution or the reaction $C(^3P_j)+C_2H_2(X\ ^1\Sigma_g^+)$ at a collision energy of 28.0 kJ mol^{-1}.

E. Flux contour maps and total relative cross sections

Figures 9–11 show the center-of-mass flux contour maps $I(\theta,E_T)\sim T(\theta)*P(E_T)$ at all three collision energies. As expected from the $T(\theta)$s, the forward peaking of the product flux with respect to the carbon beam on the relative velocity vector decreases as the relative collision energy increases and leads ultimately to a forward–backward symmetry at 45.0 kJ mol^{-1}. Integrating this flux distribution over θ, φ, E_T, and correcting for the reactant flux as well as relative reactant velocity (Table I), we find a ratio of the relative cross section of σ (8.8 kJ mol^{-1})/σ(28.0 kJ mol^{-1})=3.5±1.4. This dropping cross section with increasing collision energy correlates qualitatively with discussed bulk experiments.[25] Since no reaction channel to m/e =36 is involved, the deviation from the simple capture process $[\sigma(8.8\ \text{kJ mol}^{-1})/\sigma(28.0\ \text{kJ mol}^{-1})]_{\text{capture}}=1.3\pm0.1$ strongly indicates sterical effects when the orbiting radii fall below the van der Waals dimension of the molecule.[9] Since the fragmentation pattern of electronically excited C_2 and C_3 clusters are unknown, we cannot compute the relative cross section at E_{coll}=45.0 kJ mol^{-1}.

V. DISCUSSION

Ab initio calculations on the $C(^3P_j)/C_2H_2$ system greatly facilitate the understanding of the chemical dynamics, if the anticipated $T(\theta)$s and $P(E_T)$s are successively derived from distinct energetically accessible C_3H_2 reaction intermediates and compared with the actual experimental results. Since no triplet C_3H_2 intermediate fulfills requirements of intersystem crossing,[49,50] the discussion is limited to the triplet surface. We demonstrate that $C(^3P_j)$ interacts in the primary encounter with two acetylenic carbons to cyclopropenylidene (microchannel 1) and with one carbon atom to trans propenediylidene (microchannel 2). Propenediylidene undergoes [2,3]-H-migration to propargylene, followed by decomposition to *l*-C_3H and atomic hydrogen, whereas cyclopropenylidene fragments to *c*-C_3H and H.

A. The triplet C_3H_2 *ab initio* potential energy surface

Propargylene, hereafter HCCCH, in its $X\ ^3B$ state holds the global minimum on the triplet C_3H_2-PES with an enthalpy of formation ΔH_f° (0 K)=553.1 kJ mol^{-1},[51] Figs. 12 and 13 and Table III. The internal coordinates depict a carbon–carbon distance of 1.28 Å almost halfway between a typical double (1.34 Å) and triple (1.20 Å) bond as well as a C–C–C chain deviating by only 8.1° from linearity. These data and the torsion angle of both H atoms of 88.0° give rise to a C_2 symmetry of the 1,3 diradical and correlate with Seburg and co-workers' experimental FTIR assignment of ^{13}C substituted propargylene in argon matrices at 8 K.[52]

A second isomer, vinylidenecarbene H_2CCC, possesses C_{2v} symmetry in the lowest triplet $a\ ^3B_1$ state. The carbon–carbon lengths alternate with 1.24 Å (terminal to central) and 1.37 Å and characterize the terminal H_2CC group as olefiniclike. This interpretation gains support from a C–H distance of 1.08 Å slightly shorter than in ethylene (1.10 Å) and a HCH angle of 119° versus 117.5° in the C_2H_4 molecule. The enthalpy of formation of vinylidenecarbene ΔH_f° (0 K) =688.0 kJ mol^{-1} stands in excellent agreement with a recent experimental value of 668±30 kJ mol^{-1} calculated from ΔH_f° of singlet vinylidenecarbene via bond dissociation of the propargyl radical plus the singlet–triplet gap of vinylidenecarbene as studied from the photoelectron spectrum of the propadienylidene anion.[53]

Cyclopropenylidene *c*-C_3H_2 ($a\ ^3A$ electronic state, C_1 point group) ranks at ΔH_f° (0 K)=725.5 kJ mol^{-1}. Three carbon and one hydrogen atom span almost a plane with an 0.2° out-of-plane angle of the H atom with respect to the C_3 ring, whereas the second hydrogen atom is bent 46.1° out-of-plane. The carbon–carbon distances strongly alternate

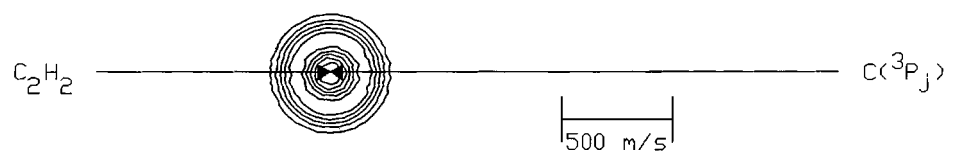

FIG. 11. Contour flux map distribution for the reaction $C(^3P_j)+C_2H_2(X\ ^1\Sigma_g^+)$ at a collision energy of 45.0 kJ mol^{-1}.

Downloaded¬12¬May¬2006¬to¬128.171.55.146.¬Redistribution¬subject¬to¬AIP¬license¬or¬copyright,¬see¬http://jcp.aip.org/jcp/copyright.jsp

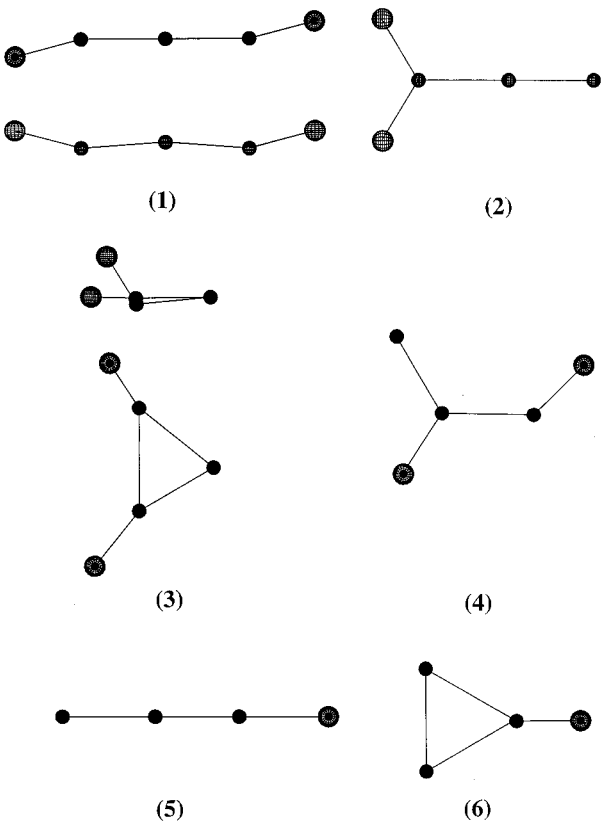

FIG. 12. *Ab initio* structures on the triplet C_3H_2 and doublet C_3H PES. Smaller sphere: carbon atom, larger sphere: hydrogen atom. Bond lengths are given in Table III. (1) propargylene, (2) vinylidenecarbene, (3) cyclopropenylidene, (4) propenediylidene, (5) linear propynylidyne, and (6) cyclopropynylidyne. Bond angles and lengths are listed in Table III.

among 1.55 Å (aliphatic), 1.45 Å (aliphatic to olefinic), and 1.30 Å (olefinic), whereas the C–H lengths range between 1.07 and 1.09 Å.

Another isomer, triplet *s-trans* propenediylidene, CHCCH,[54] (C_s symmetry; $^3A''$ electronic state) lies additionally 78.4 kJ mol^{-1} higher in energy giving ΔH_f° (0 K)=803.9 kJ mol^{-1}. As evident from the 1.35 Å (terminal to central) and 1.39 Å carbon–carbon bond lengths, the π-electron is delocalized over the carbon skeleton. A triplet *s-cis* isomer as found by Yamashita *et al.*[28] could not be confirmed even at our highest level of theory.

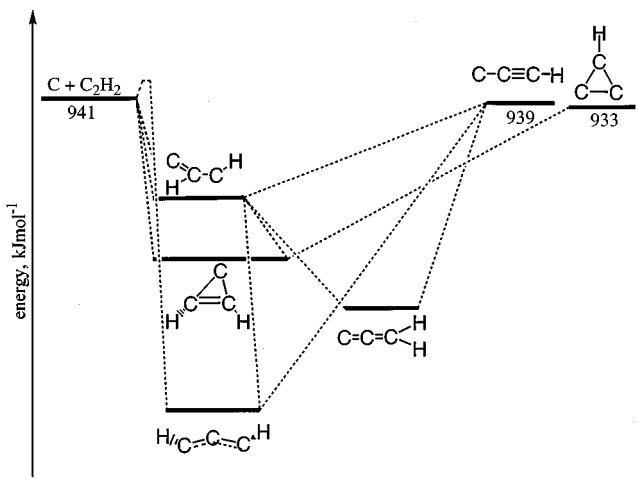

FIG. 13. Schematic representation of the lowest energy pathways on the triplet C_3H_2 PES.

B. Reaction pathways to *l*- and *c*-C_3H

The schematic energy level diagram in Fig. 13 shows three theoretically feasible, prompt reaction pathways. Insertion of $C(^3P_j)$ in the C–H bond of an acetylene molecule leads to triplet propargylene, whereas addition of the electrophile carbon atom to carbon centers on $C1$ and $C2$ atoms in C_2H_2 forms triplet cyclopropenylidene. The final pathway to triplet *s-trans* propenediylidene involves attack of two perpendicular $C(^3P_j)$-*p*-orbitals to both perpendicular π-MOs on $C1$, which might undergo consecutive [2,1]-H-migration to vinylidenecarbene, subsequent [2,3]-H-migration to propargylene, ring closure to cyclopropenylidene, or a $C2$–H bond rupture to *l*-C_3H. In addition, vinylidenecarbene might fragment via $C1$–H cleavage to *l*-$C_3H(X\ ^2\Pi_{1/2})$ or show [3,1]-H-migration to propargylene, which itself yields *l*-$C_3H(X\ ^2\Pi_{1/2})$ by $C1$–H or $C3$–H bond rupture. Finally, cyclopropenylidene can decompose directly to *c*-C_3H $(X\ ^2B_2)$ and H.

1. The isotropic microchannel

The requirement of a symmetric exit transition state confines decomposing complexes to vinylidene-carbene or propargylene. Cyclopropenylidene as well as *trans*-propenediylidene can be excluded from further discussion, since no symmetry element allows a symmetric H atom emission in θ and θ-π to account for the forward–backward symmetry of $T(\theta)$. If vinylidenecarbene existed, the decomposing complex rotated around the C_2 figure axis and formed exclusively *l*-$C_3H(X\ ^2\Pi_j)$. The linear isomer would be excited to rotations around its internuclear axis, but due to the vanishing moment of inertia, this rotation is energetically not accessible. Even accounting for the Renner–Teller effect contributes only to a quasilinear molecule, since the PES is very flat.[23,24,30] Therefore, the symmetric exit transition state results from rotation of the triplet propargylene complex around the C_2 axis. Due to the weak $\mathbf{L}-\mathbf{L}'$ coupling, our experiments cannot distinguish between an oblate and prolate exit transition state. However, future experiments probing the Λ-doublet population might resolve this puzzle.

The remaining question to be solved is the reaction pathway to triplet propargylene itself, i.e., an insertion process versus addition and subsequent hydrogen migration. Insertion of $C(^3P_j)$ into the acetylenic C–H bond can be ruled out, since only a small range of impact parameters less than 1.68 Å would contribute to the reactive scattering signal. On the other hand, bulk experiments as well as our studies indicate a dominating capture process with impact parameters as large as 3.6, 2.7, and 2.5 Å. Further, this process resembles a symmetry forbidden reaction and is expected to involve a significant entrance barrier much larger than our lowest collision

Downloaded¬12¬May¬2006¬to¬128.171.55.146.¬Redistribution¬subject¬to¬AIP¬license¬or¬copyright,¬see¬http://jcp.aip.org/jcp/copyright.jsp

TABLE III. Internal coordinates of *ab initio* equilibrium structures of triplet isomers. Parameters are designated as follows: angle 1 2 3, where 2 is the central atom; tors 1 2 3 4: torsion angle of 1 4 over the bond 2 3; outp 1 2 3 4: out-of-plane angle of the bond 4 1 with respect to the plane 2 3 4. Angles are given in degrees, bond lengths in Angstrom.

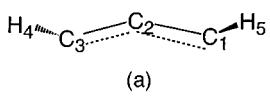

(a)

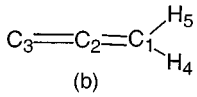

(b)

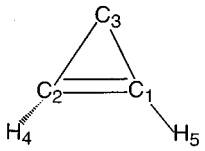

(c)

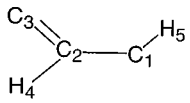

(d)

a) propargylene:		
4 3	bond length	1.067
3 2	bond length	1.279
4 3 2	angle	156.5
1 2 3	angle	171.9
4 3 1 5	tors	88.0
b) vinylidenecarbene:		
2 1	bond length	1.369
2 3	bond length	1.238
1 5	bond length	1.081
4 1 5	angle	119.0
c) cyclopropenylidene:		
2 3	bond length	1.448
1 3	bond length	1.304
1 2	bond length	1.551
2 4	bond length	1.088
1 5	bond length	1.073
4 2 1	angle	125.9
5 1 2	angle	141.1
4 3 1 2	outp	46.1
5 2 1 3	outp	0.2
d) *s-trans* propenediylidene:		
3 2	bond length	1.349
2 1	bond length	1.392
1 5	bond length	1.079
2 4	bond length	1.092
3 2 4	angle	117.1
2 1 5	angle	134.1
3 2 1	angle	121.2

energy of 8.8 kJ mol^{-1}. In strong analogy, C(^3P_j) reaction with methylacetylene exhibits no evidence of insertion into the acetylenic C–H bond.[10]

Alternatively, an interaction of two perpendicular C(^3P_j)-*p*-AOs with two acetylene π-MOs under initial C_s symmetry on the $^3A'$ surface forms a carbon–carbon σ as well as π-bond to *s-trans* propenediylidene. This pathway involves a maximum orbital overlap and opens a large range of impact parameters for reactive encounters.[10] A subsequent [2,3]-H-migration in *s-trans* propenediylidene yields propargylene which must rotate around its C_2 figure to explain the isotropic, forward–backward symmetric $T(\theta)$. Therefore, no symmetry element is conserved during the reaction and the initial C_s approach symmetry is reduced to C_1. Hence, the reaction proceeds on the ^3A surface to yield l-$C_3H(X\ ^2\Pi_j)$ and H($^2S_{1/2}$) via C–H bond rupture.

This ideal initial C_s approach symmetry to propenediylidene preserves the C–C–C plane as a symmetry element. Since the initial orbital angular momentum becomes the total angular momentum of the initially formed collision complex, *s-trans* propenediylidene rotates in a plane almost perpendicular to **L** around its *C* axis. A slight off-plane approach of the carbon atom toward acetylene under C_1 symmetry can excite *B* rotations as well. Unfortunately, experimental data cannot prove the *s-trans* structure of the propenediylidene isomer explicitly. But similar reactions of C_2H_2 with CH_3[54] and H[55] lead solely to intermediates in which the former acetylenic hydrogen atoms are located

Downloaded¬12¬May¬2006¬to¬128.171.55.146.¬Redistribution¬subject¬to¬AIP¬license¬or¬copyright,¬see¬http://jcp.aip.org/jcp/copyright.jsp

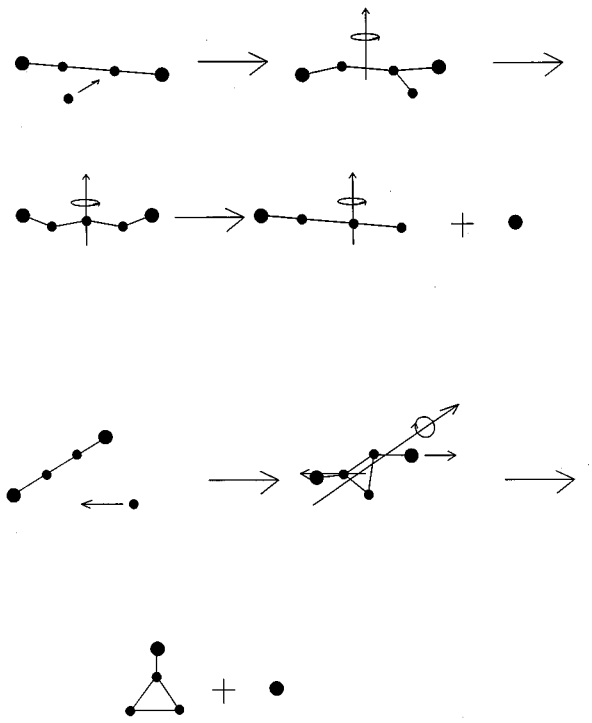

FIG. 14. Schematic reaction pathways of $C(^3P_j)$ with $C_2H_2(X\ ^1\Sigma_g^+)$ on the triplet surface. Upper: reaction to $1-C_3H$ via *s-trans* propadienylidene and propargylene. Lower: reaction to *c*-C_3H via triplet cyclopropenylidene.

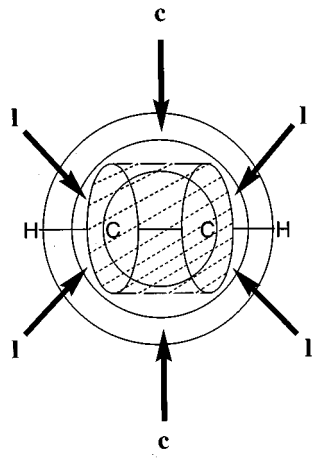

FIG. 15. Schematic representation of sterical effects on the reaction $C(^3P_j)+C_2H_2(X\ ^1\Sigma_g^+)$ with decreasing orbiting radii. ''c'' denotes preferential attack to form cyclopropenylidene, and ''l'' propadienylidene.

trans to each other, and the reaction proceeds very likely through the *s-trans* isomer.

2. The forward-scattered microchannel

The strongly forward-scattered microchannel 2 exhibits a strong $\mathbf{L}-\mathbf{L}'$ correlation and requires that the incorporated carbon atom and the leaving hydrogen must be located on opposite sites of the rotation axis in the decomposing triplet C_3H_2 complex. This condition alone limits potential fragmenting triplet complexes to propenediylidene rotating around its *A* axis, propargylene (*A*/*C*-like rotations), cyclopropenylidene (*A*/*C*-like rotations), and vinylidenecarbene (*B*-like rotations). Since the reaction follows direct, stripping dynamics and the $T(\theta)$s strongly peak at $\theta=0^0$, a large range of impact parameters contribute to the reactive scattering signal.[26] Therefore, $C(^3P_j)$ insertion into the acetylenic C–H bond to propargylene can be excluded as well; the absence of insertion intermediates in reaction (10) was already outlined in the previous paragraph. Therefore, microchannel 2 has to proceed via propadienylidene or cyclopropenylidene.

The deviation of the energy dependent relative cross sections at 8.8 and 28.0 kJ mol^{-1} from the classical capture theory resolves the reaction dynamics. Although the detailed structure of the molecule does not play a role within the simple capture framework, chemical forces must be taken into account, if the capture radius is on the order of the van der Waals dimensions of the acetylene molecule. This leads to an alteration of the simple orbiting picture and focusses on the electronic structure of the acetylene molecule. As the orbiting radius decreases with rising collision energy, reactive encounters from radii exceeding the symmetric π-cloud to form cyclopropenylidene, Fig. 15, become more and more unlikely, and are shifted toward orbits in which the π-cloud can be attacked sideways to yield preferentially the propenediylidene isomer. This model explains a decreasing cross section and hence forward peaking center-of-mass angular distribution as the collision energy rises and further underlines the geometry limited formation of the triplet *c*-C_3H_2 isomer. Our conclusion is consistent with typical time scales for hydrogen migrations; even the fastest known H rearrangement from vinylidene to acetylene takes ca. 1 ps,[57] one order of magnitude more than the typical 0.1 ps required to explain the direct reaction dynamics; therefore, no hydrogen migration from propenediylidene to vinylidene or propargylene contributes to the forward scattered $T(\theta)$. As mentioned above, a decomposing propenylidene complex itself excited to *A*-like rotations would explain the forward peaked $T(\theta)$, but fails to account for the decreasing cross section with increasing collision energy.

The assignment of a triplet cyclopropenylidene enables us to identify rotations around the A-axis. Figure 14 outlines this approach geometry of $C(^3P_j)$ toward the acetylene molecule. As evident, the second out-of-plane H atom is nearly perpendicular to the plane and can likely be ejected almost instantaneously after C–H bond rupture backwards with respect to the carbon trajectory, whereas the *c*-C_3H proceeds in the forward direction. These direct stripping dynamics account for the strongly forward peaked $T(\theta)$s of microchannel 2.

C. Exit transition states

The collision energy dependent shapes of the $P(E_T)$s unveil valuable information on the chemical dynamics between the moment of the triplet C_3H_2 complex formation and the separation into products. All $P(E_T)$s peak between 5 and 16 kJ mol^{-1}, suggesting a loose exit transition state without any significant interaction between the departing C_3H isomer

Downloaded¬12¬May¬2006¬to¬128.171.55.146.¬Redistribution¬subject¬to¬AIP¬license¬or¬copyright,¬see¬http://jcp.aip.org/jcp/copyright.jsp

and H atom beyond the critical configuration. This framework should correlate with only minor geometry changes from the decomposing triplet C_3H_2 complexes to l/c-C_3H isomers, as evident from the molecular dimensions. Compared to triplet propargylene, the C–C and C–H distances alter by less than 0.07 Å in l-C_3H, i.e., virtually unchanged C–H bond, a C–C bond distance change from 1.28 Å to 1.24 Å and 1.35 Å, respectively, a bending angle of the three propargylene carbon atoms deviating by only 8.1° from the linear geometry, and a H–C–C bond angle widened from 156.5° to 180°. Larger geometry changes up to about 0.3 Å are found in the cyclic C_3H isomer as compared to triplet c-C_3H_2: alternating C–C distances of 1.45, 1.30, and a C–H distance of 1.07 Å show almost identical C–C lengths of 1.37 and 1.38 Å in c-C_3H, and the C–H bond increases slightly from 1.07 Å to 1.08 Å. Likewise, the three carbon and $H1$ of c-C_3H_2 are almost in one plane as found in the C_{2v} symmetric c-C_3H isomer. The order of magnitude of the exit barrier of 5–16 kJ mol^{-1} is consistent, if we compare to $P(E_T)$s of reaction (10) peaking at 30–60 kJ mol^{-1}. Here, a simple, nearly barrierless bond rupture of the C–H bond in the CH_3 group would localize electron density on the terminal carbon atom. The accompanying electron delocalization over the C_4 carbon skeleton, however, induces an additional change in electron density to an increased exit barrier. These findings associate with simple correlation diagrams on the ^3A surface under C_1 symmetry and show a correlation of the ground state cyclopropenylidene as well as propargylene surface with ground state l/c-C_3H.

V. COMPARISON WITH RELATED SYSTEMS

A. $C(^3P_j)+CH_3CCH(X^1A_1)$

The chemical dynamics to l-C_3H show strong similarities with the reaction of $C(^3P_j)+CH_3CCH$.[10] Here, $C(^3P_j)$ attacks both perpendicular acetylenic π-MOs to triplet *s-trans* methylpropenediylidene as well. The initial collision complex undergoes a similar [2,3]-H-migration to methylpropargylene which decomposes to n-C_4H_3 and H. Further, recent matrix studies via FTIR spectroscopy show transformation of propenediylidene to propargylene upon heating the argon matrix from 10 K to 36 K and imply a barrier less than 1 kJ mol^{-1} for the involved H migration.[58] This low barrier is consistent with the [2,3]-H-migration prevailing even at highest collision energies of 45.0 kJ mol^{-1}. The increased exit barrier of 30–60 kJ mol^{-1} to n-C_4H_3 [reaction (10)] versus only 5–16 kJ mol^{-1} to l-C_3H correlates with a stronger electron reorganization from the decomposing triplet methylpropargylene complex as compared to triplet propargylene to the products. A triplet methylcyclopropenylidene collision complex analogous to unsubstituted triplet c-C_3H_2, however, could not be identified. Here, the methyl group very likely reduces the cone of acceptance and screens approach geometries to form the triplet c-C_4H_4 intermediate.[10,26]

The alternative interpretation of a long-lived C_3H_2 collision complex contributing to a symmetric $T(\theta)$ can be dismissed, if we compare the center-of-mass angular distribution of this reaction with those of $C(^3P_j)+CH_3CCH(X\ ^1A_1)$. As obvious from the potential energy well depth of all triplet C_3H_2 isomers relative to the reactants and products, triplet propargylene is expected to hold the highest lifetime. Since the fragmenting methylpropargylene complex shows an osculating behavior at 33.2 kJ mol^{-1}, the reduced number of 9 (propargylene) versus 18 (methylpropargylene) vibrational modes suggests a short-lived propargylene complex with a lifetime less than its rotational period of 1.5–2.7 ps around the C_2 symmetry axis, at least at a collision energy of 45.0 kJ mol^{-1}. Due to the symmetric exit transition state to c-C_3H, no explicit information on the propargylene lifetime can be derived. However, future experiments of $C(^3P_j)$ with partially deuterated acetylene, C_2HD, are aimed to break the C_2 symmetry of the propargylene intermediate. This approach explicitly reveals the transition from a long-lived to an osculating complex with increasing collision energy as found very recently for the reaction of atomic nitrogen with acetylene to a triplet HCCN isomer and atomic hydrogen[59] as the collision energy rises from 12.6 to 37.7 kJ mol^{-1}:

$$N(^2D)+C_2H_2(X\ ^1\Sigma_g^+)\rightarrow HCCN+H. \tag{12}$$

B. $O(^3P_j)+C_2H_2(X\ ^1\Sigma_g^+)$

The dynamics of the reaction $O(^3P_j)$ with $C_2H_2(X\ ^1\Sigma_g^+)$ were elucidated recently in our group[60] and depict two channels initiated via attack of the oxygen atom to a π-orbital of one acetylenic carbon to *s-trans* HCOHC on the $^3A''$ surface. This long-lived intermediate either fragments directly to the ketenyl radical, $HCCO(X\ ^2A'')$, and H or undergoes [1,2]-H-migration to triplet ketene prior to $CH_2(X\ ^3B_1)$ and $CO(X\ ^1\Sigma^+)$ decomposition. As outlined in Sec. IV B, a direct C–H bond rupture of *s-trans* propenediylidene to H and l-C_3H is energetically not accessible, since the l-C_3H had to rotate around its internuclear axis. The ketenyl radical, however, possesses a bent geometry in its electronic ground state, and A-like rotations can be excited. Further, a hydrogen shift from propenediylidene to triplet vinylidenecarbene could be covered, but the subsequent exit channel to CH_2 $(X\ ^3B_1)$ and C_2 $(X\ ^1\Sigma_g^t)$ similar to the $CH_2(X\ ^3B_1)$ and $CO(X\ ^1\Sigma^+)$ channel cannot be opened up at collision energies up to 45.0 kJ mol^{-1} applied in our experiments (Table I). Likewise, a hydrogen shift similar to a [2,3]-H-rearrangement in propenediylidene to form propargylene would yield triplet hydroxy-acetylene, but the keto-enol equilibrium is expected to favor the HCOHC keto structure. Finally, formation of a cyclic triplet oxirane collision complex might involve an entrance barrier resulting from electrostatic interaction of the doubly occupied p-orbital with the closed shell acetylene molecule. Compared to the $C(^3P_j)+C_2H_2(X\ ^1\Sigma_g^t)$ encounter, this p-orbital is vacant, and the electrostatic interaction is eliminated.

VI. ASTROPHYSICAL IMPLICATIONS

The cyclic and linear C_3H isomers have both been identified toward the dark molecular cloud TMC-1 and the carbon star IRC+10216. In dark clouds, typical ratios of the cyclic versus the linear isomer are near unity, but decrease to

Downloaded¬12¬May¬2006¬to¬128.171.55.146.¬Redistribution¬subject¬to¬AIP¬license¬or¬copyright,¬see¬http://jcp.aip.org/jcp/copyright.jsp

0.2 ± 0.1 around the carbon star. Especially the circumstellar shell at distances between 10^{14} and 10^{15} m contains a C_2H_2 as well as $C(^3P_j)$ reservoir,[61] and formation of C_3H via neutral–neutral reaction very likely takes place. Our results correlate qualitatively with these observations. Dark clouds hold typical averaged translational temperatures of 10 K, whereas circumstellar shells around carbon stars are heated up to about 4000 K. Since 10 000 K are roughly equivalent to 100 kJ mol^{-1}, this gives a mean translational energy of about 0.01 and 40 kJ mol^{-1} in dark clouds and outflow of carbon stars, respectively. Therefore, both isomers are expected to exist in dark, molecular clouds, but the $[c\text{-}C_3H]/[l\text{-}C_3H]$ ratio should decrease in IRC+10216, as found in astronomical surveys, since less c-C_3H should be produced as the averaged translational temperature increases. Therefore, a common acetylene precursor to interstellar c/l-C_3H radicals via atom–neutral reaction with $C(^3P_j)$ seems reasonable.

VII. CONCLUSIONS

The reaction between ground state carbon atoms, $C(^3P_j)$, and acetylene, $C_2H_2(X\ ^1\Sigma_g^+)$, was studied at three average collision energies of 8.8, 28.0, and 45.0 kJ mol^{-1} using the crossed molecular beams technique. Reaction dynamics inferred from TOF spectra and LAB distributions combined with our *ab initio* calculations suggest two microchannels, initiated by addition of $C(^3P_j)$ either to one carbon atom of the acetylene molecule yielding *s-trans* propenediylidene (microchannel 1) or two carbon atoms forming triplet cyclopropenylidene (microchannel 2) via loose transition states located at their centrifugal barriers. Propenediylidene rotates around its B/C axis and undergoes [2,3]-H-migration to propargylene, followed by C–H bond cleavage via a symmetric exit transition state to l-$C_3H(X\ ^2\Pi_{1/2})$+H. These dynamics supply a collision energy invariant, isotropic center-of-mass angular distribution as well as a weak **L-L′** correlation. A strongly forward scattered microchannel 2 shows a significant **L-L′** correlation, but is quenched with rising collision energy. Its chemical dynamics involve a short-lived triplet cyclopropenylidene complex excited to A-like rotations which subsequently fragments to c-$C_3H(X\ ^2B_2)$ and H through a loose transition state located 6-12 kJ mol^{-1} above the products.

The explicit identification of l-$C_3H(X\ ^2\Pi_j)$ and c-$C_3H(X\ ^2B_2)$ under single collision conditions represents a one-encounter pathway to build up hydrocarbon radicals in the interstellar medium and represents a more realistic synthetic route to interstellar C_3H isomers than postulated ion–molecule reaction networks. Energy dependent branching ratios of the linear versus cyclic isomer correlate qualitatively with astronomical observations and explain the c-C_3H/l-C_3H ratio of one in the molecular cloud TMC−1, but a reduced value of 0.2 in outflow of the carbon star IRC+10216. Hence, a common acetylene precursor to interstellar c/l-C_3H via the atom neutral reaction with atomic carbon seems highly likely. Further, the triplet C_3H_2 intermediates propadienylidene and cyclopropenylidene might resemble those C_3H_2 isomers trapped as singlet dimethylthioesters in oxidative acetylene flames[33] and suggests reactive intermediates in the CVD process to synthetic diamonds.[31,32]

ACKNOWLEDGMENTS

R.I.K. and C.O. are indebted the Deutsche Forschungsgemeinschaft (DFG) for post-doctoral fellowships. One of us, C.O., thanks Professor Jürgen Gauss, Universität Mainz, Germany, and Dr. Dage Sundholm, University of Helsinki, Finland, for assistance in using the ACES II program system and for providing a DEC version of this package. This work was further supported by the Director, Office of Energy Research, Office of Basic Energy Sciences, Chemical Sciences Division of the U.S. Department of Energy under Contract No. DE-AC03-76SF00098.

[1] C. A. Gottlieb, J. M. Vrtilek, E. W. Gottlieb, P. Thaddeus, and A. Hjalmarson, Ap. J. **294**, L55 (1985).
[2] S. Yamamoto and S. Saito, J. Chem. Phys. **101**, 5484 (1994).
[3] S. Yamamoto, S. Saito, M. Ohishi, H. Suzuki, S. I. Ishikawa, N. Kaifu, and A. Murakami, Ap. J. **322**, L55 (1987).
[4] S. Green, Ap. J. **240**, 962 (1980).
[5] S. Yamamoto and S. Saito, Ap. J. **363** L13 (1990).
[6] S. C. Madden, in *Chemistry in Space*, edited by J. M. Greenberg and V. Pirronello (Kluwer, Dordrecht, 1991), p. 437.
[7] S. D. Prodnuk, C. H. DePuy, and V. M. Bierbaum, Int. J. Mass Spectrom. **100**, 693 (1990).
[8] R. I. Kaiser, Y. T. Lee, and A. G. Suits, J. Chem. Phys. **103**, 10395 (1995).
[9] R. I. Kaiser, Y. T. Lee, and A. G. Suits, J. Chem. Phys. **105**, 8705 (1996).
[10] R. I. Kaiser, D. Stranges, Y. T. Lee, and A. G. Suits, J. Chem. Phys. **105**, 8721 (1996).
[11] F. J. Lovas, R. D. Suenram, T. Ogata, and S. Yamamoto, Ap. J. **399**, 325 (1992).
[12] S. Yamamoto, S. Saito, H. Suzuki, S. Deguchi, N, Kaifu, S. I. Ishikawa, and M. Ohishi, Ap. J. **348**, 363 (1990).
[13] Q. Jiang, C. M. Rittby, and W. R. M. Graham, J. Chem. Phys. **99**, 3194 (1993).
[14] C. C. Mangum and A. Wootten, Astron. Astrophys. **239**, 319 (1990).
[15] S. Green, Ap. J. **240**, 962 (1980).
[16] H. Yamagishi, H. Taiko, S. Shimogawara, A. Murakami, T. Noro, and K. Tanaka, Chem. Phys. Lett. **250**, 165 (1990).
[17] C. A. Gottlieb, T. C. Killian, P. Thaddeus, P. Botschwina, J. Fluegge, and M. Oswald, J. Chem. Phys. **98**, 4478 (1994).
[18] P. Thaddeus, C. A. Gottlieb, R. Mollaaghababa, and J. M. Vrtilek, J. Chem. Faraday Soc. **89**, 2125 (1989).
[19] J. A. Montgomery, J. W. Ochterski, and G. A. Peterson, J. Chem. Phys. **101**, 5900 (1994).
[20] J. F. Stanton, Chem. Phys. Lett. **237**, 20 (1995).
[21] K. Aoki, K. Hashimoto, S. Ikuta, and A. Murakami, Ap. J. (submitted).
[22] J. Takahashi and K. Yamashita, presented to the Annual Spring Meeting of the Chemical Society of Japan.
[23] M. Kanada, S. Yamamoto, S. Saito, and Y. Osamura, J. Chem. Phys. **104**, 2192 (1996).
[24] G. Herzberg, *Molecular Spectra and Electronic Structure of Polyatomic Molecules* (Krieger, Malabar, 1991).
[25] D. C. Clary, N. Haider, D. Husain, and M. Kabir, Ap. J. **422**, 416 (1994).
[26] R. D. Levine, and R. B. Bernstein, *Molecular Reaction Dynamics and Chemical Reactivity* (Oxford University Press, Oxford, 1987).
[27] Q. Liao and E. Herbst, Ap. J. **444**, 694 (1995).
[28] J. Takahashi and K. Yamashita, J. Chem. Phys. **104**, 6613 (1996).
[29] R. I. Kaiser, C. Ochsenfeld, M. Head-Gordon, Y. T. Lee, and A. G. Suits, Science **274**, 1508 (1996).
[30] C. Ochsenfeld, R. I. Kaiser, Y. T. Lee, A. G. Suits, and M. Head-Gordon, J. Chem. Phys. (in press).
[31] F. G. Celii and J. E. Butler, Annu. Rev. Phys. Chem. **42**, 643 (1991).
[32] D. C. Harris, Naval Res. Rev. **3**, 1 (1992).

Downloaded¬12¬May¬2006¬to¬128.171.55.146.¬Redistribution¬subject¬to¬AIP¬license¬or¬copyright,¬see¬http://jcp.aip.org/jcp/copyright.jsp

[33] M. Hausmann and K. H. Homann, Ber. Bunsenges. Phys. Chem. **94**, 1312 (1990).
[34] Y. T. Lee, J. D. McDonald, P. R. LeBreton, and D. R. Herschbach, Rev. Sci. Instrum. **40**, 1402 (1969).
[35] R. I. Kaiser and A. G. Suits, Rev. Sci. Instrum. **66**, 5405 (1995),
[36] R. I. Kaiser, Y. T. Lee, and A. G. Suits (unpublished).
[37] M. S. Weiss, Ph.D. thesis, University of California, Berkeley (1986).
[38] K. Raghavachari, G. W. Trucks, J. A. Pople, and M. Head-Gordon, Chem. Phys. Lett. **157**, 479 (1989).
[39] J. Gauss, W. J. Lauderdale, J. F. Stanton, J. D. Watts, and R. J. Bartlett, Chem. Phys. Lett. **182**, 207 (1991).
[40] J. D. Watts. J. Gauss, and R. J. Bartlett, J. Chem. Phys. **98**, 8718 (1993).
[41] J. D. Watts, J. Gauss, and R. J. Bartlett, Chem. Phys. Lett. **200**, 1 (1992).
[42] ACES II, an *ab initio* program system written by J. F. Stanton, J. Gauss, J. D. Watts, W. J. Lauderdale, R. J. Bartlett. Quantum Theory Project, University of Florida, Gainesville (1992).
[43] J. F. Stanton, J. Gauss, J. D. Watts, W. J. Lauderdale, and R. J. Bartlett, Int. J. Quant. Chem. **6**, 879 (1992).
[44] J. Cizek, J. Paldus, J. Chem. Phys. **47**, 3976 (1967).
[45] A. Schäfer, H. Horn, and R. Ahlrichs, J. Chem. Phys. **97**, 2571 (1992).
[46] T. H. Dunning, J. Chem. Phys. **90**, 1007 (1989).
[47] W. B. Miller, S. A. Safron, and D. R. Herschbach, Discuss. Faraday Soc. **44**, 108, 291 (1967).
[48] W. B. Miller, Ph.D. thesis, Harvard University, Cambridge (1969).
[49] N. J. Turro, *Modern Molecular Photochemistry* (University Science Books, Mill Valley, 1991).
[50] A. P. Scott, R. H. Nobes, H. F. Schaefer, and L. Radom, J. Am. Chem. Soc. **116**, 10159 (1994).
[51] Enthalpies of formations were calculated by subtracting the *ab initio* reaction enthalpies from the $C(^3P_j)$ and C_2H_2 reactants to triplet C_3H_2 isomers from the literature data of the reactants as given in *Handbook of Chemistry and Physics* (CRC, Boca Raton, 1995).
[52] R. A. Seburg and R. J. McMahon, Angew. Chem. **107**, 2198 (1995).
[53] M. S. Robinson, M. L. Polak, V. M. Bierbaum, C. H. DePuy, and W. C. Linerberger, J. Am. Chem. Soc. **117**, 6766 (1995).
[54] ''*trans*'' refers to the position of both hydrogen atoms with respect to the former acetylenic carbon–carbon bond, whereas ''s'' denotes the new single bond.
[55] V. Barone and L. Orlandini, Chem. Phys. Lett. **246**, 45 (1995).
[56] L. B. Harding, H. F. Wagner, J. M. Bowman, and G. C. Schatz, J. Phys. Chem. **86**, 4312 (1982).
[57] T. Carrington, L. M. Hubbard, H. F. Schaefer, and W. H. Miller, J. Chem. Phys. **80**, 4347 (1984).
[58] J. W. Huang and W. R. M. Graham, J. Chem. Phys. **93**, 1583 (1990).
[59] P. Casavecchia, University of Perugia, Italy (private communication).
[60] A. M. Schmoltner, P. M. Chu, and Y. T. Lee, J. Chem. Phys. **91**, 5365 (1989).
[61] J. Keene, K. Young, T. G. Phillips, and T. H. Büttgenbach, Ap. J. **415**, L131 (1993).

Downloaded¬12¬May¬2006¬to¬128.171.55.146.¬Redistribution¬subject¬to¬AIP¬license¬or¬copyright,¬see¬http://jcp.aip.org/jcp/copyright.jsp